Nuclear Inst. and Methods in Physics Research, A 1029 (2022) 166418

Contents lists available at ScienceDirect

Nuclear Inst. and Methods in Physics Research, A

journal homepage: www.elsevier.com/locate/nima

Technical Notes

A new active vibration control method of double crystal monochromator based on FuLMS-ADRC hybrid algorithm

Bai Yang [a,b], Gong Xuepeng [a,*], Lu Qipeng [a,*], Song Yuan [a], Wang Dazhuang [a], Peng Zhongqi [a], Zhang Zhen [a], Mao Qijun [a,b], Ma Tianyu [a,b]

[a] State key Laboratory of Applied Optics, Changchun Institute of Optics, Fine Mechanics and Physics, Chinese Academy of Sciences, Changchun 130033, China
[b] University of Chinese Academy of Sciences, Beijing 100049, China

ARTICLE INFO

Keywords:
Synchrotron radiation
Double-crystal monochromator
FuLMS-ADRC hybrid algorithm
Active vibration control

ABSTRACT

The stability of crystal monochromator is the main technical bottleneck of the overall performance of X-ray beam. Generally, in the field of synchrotron radiation, the stability of double crystal monochromator (DCM) is guaranteed by passive vibration control method. In this paper, we propose a new active vibration control method of DCM based on FuLMS-ADRC hybrid algorithm. The angular stability of DCM in the pitch direction is improved from 352.24 nrad to 3.07 nrad (LN_2 cooling cycle) by the active vibration control method. This new active vibration control method based on FuLMS-ADRC hybrid algorithm not only provides a new technical scheme to improve the overall performance of hard X-ray beam, but also is of great significance to realize the nano-radian stability index of the fourth-generation synchrotron radiation beam optical equipment.

1. Introduction

BSL-2 macromolecular crystallography beam line (P2, BL10U2) is one of the phase II beam line stations established by SSRF, which is specially used to study the structure of virus particles by X-ray crystal diffraction. The low temperature cooled DCM of BSL-2 beam line station is used to separate the required narrow wavelength beam from synchrotron radiation X-ray spectrum and focus the beam at the sample position.

The Bragg angle stability of DCM is very important for beam position, flux and resolution of hard X-ray beam. At present, the angle stability of the actual DCM is required to be 30~50 nrad. The main factor affecting the stability of DCM is the cooling flow of LN_2 [1]. At present, the stability of DCM is mainly solved by passive vibration control in synchrotron radiation laboratories all over the world. Spring-8 has designed a low vibration flexible tube, which stabilizes the coolant flow by covering the ripple of the flexible tube with alumina fiber fabric to ensure the stability of the crystal monochromator [2]; ESRF proposes a new generation of mirror system to suppress vibration and ensure ultra-high thermal stability [3]. SSRF optimizes the 2nd attitude fine-tuning mechanism of DCM and the circuit of LN_2 cooling system. The stability in the pitch direction meets the 300 nrad/2 h stability requirements in the user experiment of macromolecular crystallography beam line (P2, BL10U2) [4,5]. The 2nd attitude fine-tuning mechanism is shown in Fig. 1 and the four-axis flexure hinge is shown in Fig. 2.

In this paper, aiming at the problem of micro-vibration in the pitch direction of the 2nd crystal, we design the four-axis flexure hinge AVC (active vibration control) system of the attitude fine-tuning mechanism of the DCM based on the FuLMS-ADRC hybrid algorithm. The results show that the displacement amplitude of the DCM in the pitch direction is reduced to 3.07 nrad by this active vibration control method under the LN_2 cooling cycle. This new active vibration control method based on FuLMS-ADRC hybrid algorithm provides an innovative technical scheme for the upgrading of DCM in synchrotron radiation facilities. At the same time, it is of great significance for the development of ultra-high stable DCM in X-beam line stations of synchrotron radiation facilities all over the world.

2. Experimental setup

2.1. Design of AVC system

The dynamic equation of four-axis flexure hinge is described based on the second kind of Lagrange equation [6]. The frequency response function curve of four-axis flexure hinge is shown in Fig. 3. Obviously, the natural frequency of four-axis flexure hinge is 452 Hz. FuLMS (filter-U Least Mean square) algorithm has the advantages of suppressing the instability of control system caused by vibration feedback and low-order filter structure [7]. ADRC (active disturbance rejection control) control algorithm is widely used in the field of vibration control. It shows strong robustness to the uncertainty of system parameters and uncertain external disturbances [8]. We propose a new active vibration

* Corresponding authors.
E-mail addresses: gongxuepeng120@foxmail.com (X. Gong), Luqipeng@126.com (Lu Q.).

https://doi.org/10.1016/j.nima.2022.166418
Received 18 November 2021; Received in revised form 3 January 2022; Accepted 23 January 2022
Available online 9 February 2022

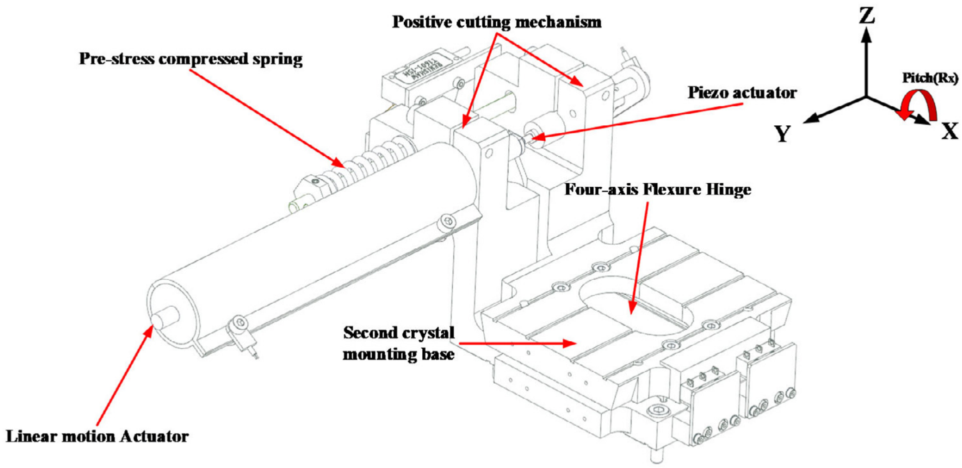

Fig. 1. Mechanism for the fine-tune along pitch direction of the 2nd crystal.

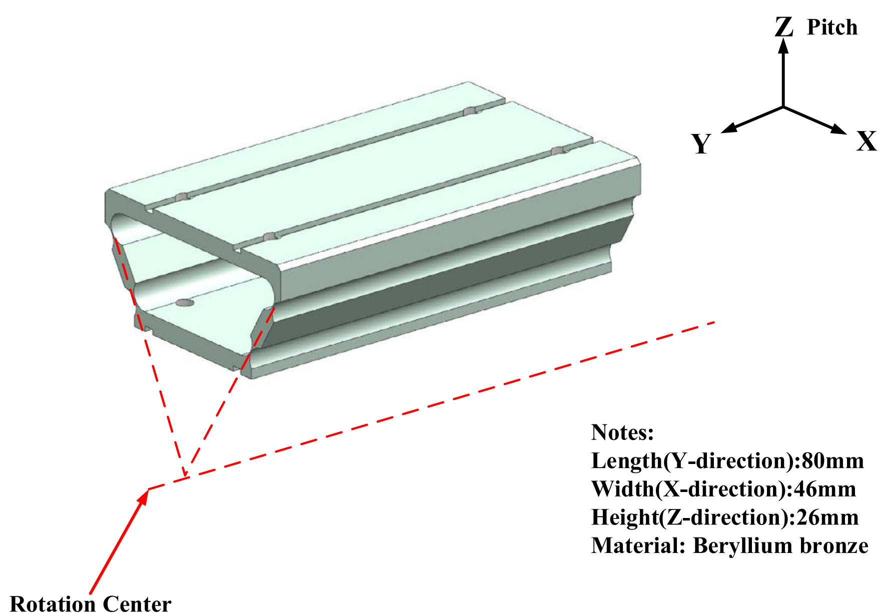

Fig. 2. Structure of the four-axis flexure hinge.

control method based on FuLMS-ADRC hybrid algorithm, which can reduce the interference of error signal to FuLMS control system and further improve the convergence accuracy of system. The structure diagram of active control system based on FuLMS-ADRC hybrid algorithm is shown in Fig. 4.

The calculation formula of the control system based on FuLMS-ADRC hybrid algorithm is as follows:

$$X(n) = [x(n), \ldots, x(n-P+1)] \tag{1}$$

$$Y_S(n) = [y_s(n), \ldots, y_s(n-Q+1)] \tag{2}$$

$$W_1(n) = [w_{10}(n), \ldots, w_{1P-1}(n)] \tag{3}$$

$$W_2(n) = [w_{20}(n), \ldots, w_{2Q-1}(n)] \tag{4}$$

$$d_n = X(n) * P(n) \tag{5}$$

$$y_s(n) = \left[y_1(n) + y_2(n)\right] * S(n) \tag{6}$$

$$y_1(n) = X(n) * W_1(n) \tag{7}$$

$$y_2(n) = y_1(n-1) * W_2(n) \tag{8}$$

$$y'(n) = y_1(n-1) * S'(n) \tag{9}$$

$$e_1(n) = d(n) - y_s(n) \tag{10}$$

$$w_1(n+1) = w_1(n) + 2\rho x'(n) e_1(n) \tag{11}$$

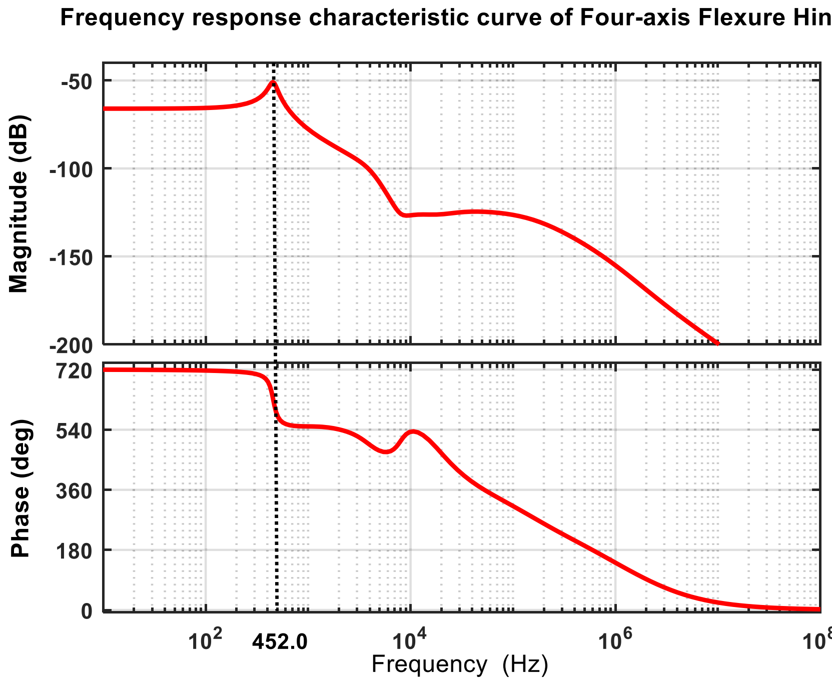

Fig. 3. The frequency response function curve of the Four-axis flexure hinge.

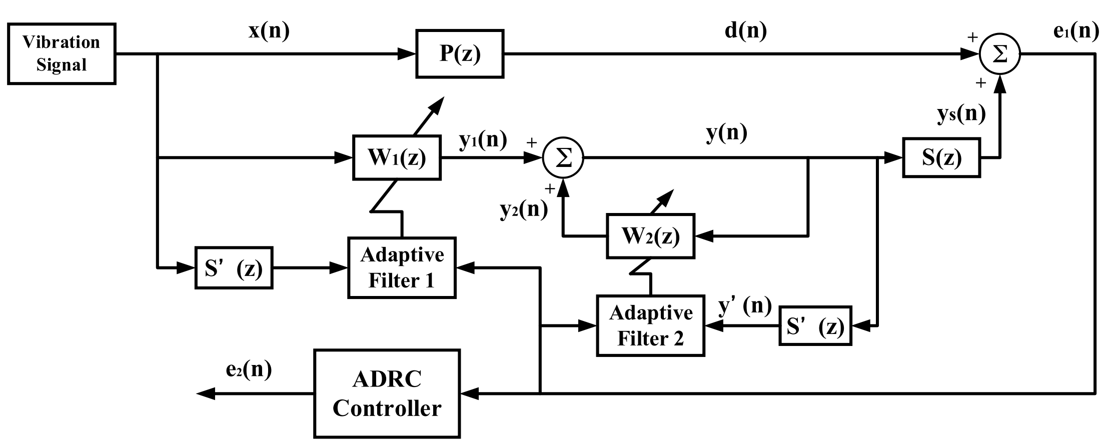

Fig. 4. Structure of FuLMS-ADRC hybrid algorithm.

$$w_2(n+1) = w_2(n) + 2\mu y'(n) e_1(n) \tag{12}$$

$$\left\{\begin{matrix} e_1' = e_{11}(k) - z_1(k) \\ e_2' = e_{12}(k) - z_2(k) \\ u_0 = \beta_{01}\mathrm{fal}\left(e_1', \alpha_1, \delta\right) + \beta_{02}\mathrm{fal}(e_1', \alpha_1, \delta) \\ e_2(k) = u_0 - \frac{z_3(k)}{b} \end{matrix}\right\} \tag{13}$$

$$\mathrm{fal}(\varepsilon, \alpha, \delta) = \begin{cases} |\varepsilon|^{\alpha} sgn(\varepsilon), & |\varepsilon| > \delta \\ \frac{\varepsilon}{\delta^{1-\alpha}}, & |\varepsilon| \le \delta \end{cases} \quad \delta > 0 \tag{14}$$

where $X(n)$ is the input vibration signal vector; $Y_S(n)$ is the anti-vibration signal; W_1 is feedforward filter; W_2 is feedback filter; P is the length of feedforward filter; Q is the feedback filter length; d_n is the desired signal passing through the primary channel; $S(n)$ is the transfer function of the secondary channel; $S'(n)$ is the estimation of the secondary channel; $e_1(n)$ is the output error signal of FuLMS controller; ρ, μ is the iteration step; "*" indicates convolution; $e_{11}(k), e_{12}(k)$ is transition signal of $e_1(n)$; $z_1(k), z_2(k)$ is the state estimation of $e_2(k)$; α is a nonlinear factor; δ is the filter coefficient; β_{01}, β_{02} is the gain coefficient; ε is the state feedback error; b is the gain of system control quantity.

3. Results and discussions

The work frequency of DCM in SSRF P2 experimental station at Bragg@12.66kev is shown in Table 1 [9]. The vibration source curve is shown in Fig. 5. Based on formula (1)~(14), the simulation calculation is carried out on Simulink platform.

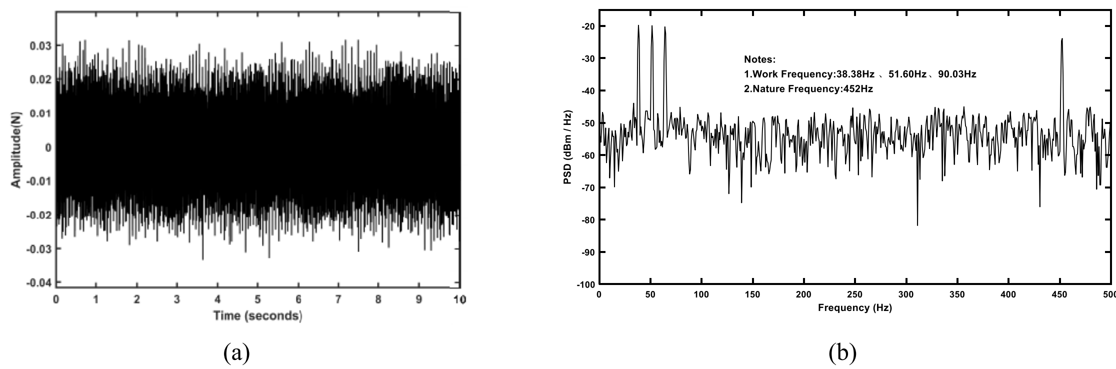

Fig. 5. Vibration source curve. (a) time-domain (b) frequency-domain.

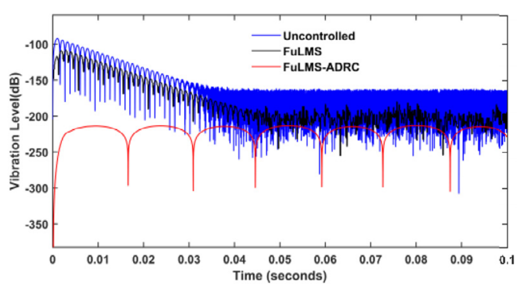

Fig. 6. The vibration level of displacement signal under step-disturbance.

Table 1
The work frequency of DCM in SSRF P2 experimental station at Bragg@12.66 kev.

Mode	Frequency (Hz)				
LN_2	38.38	51.60	64.30	–	–

Table 2
The maximum value of vibration level under step-disturbance.

Method	Uncontrolled	FuLMS	FuLMS-ADRC
Vibration Level (dB)	−91.75	−108.4	−213.3

3.1. *time–frequency analysis*

The vibration level of displacement signal under step-disturbance is shown in Fig. 6. The displacement signal of four-axis flexure hinge in the pitch direction under step-disturbance is shown in Fig. 7. The maximum value of vibration level is shown in Table 2. The active vibration control method based on FuLMS-ADRC hybrid algorithm can reduce the peak-to-peak value of displacement signal in the pitch direction of four-axis flexure hinge by 99.98%; the maximum value of vibration level decreases by 121.55 dB.

The time-domain signal displacement of four-axis flexure hinge in the pitch direction under random disturbance is shown in Fig. 8. The RMS value of angular displacement of four-axis flexure hinge in the pitch direction is shown in Table 3. The vibration level of displacement signal is shown in Fig. 9. The maximum value of vibration level is shown in Table 4. The active vibration control method based on FuLMS-ADRC hybrid algorithm reduces angular displacement of four-axis flexure hinge in the pitch direction by 99.13%. In particular, the angular stability in the pitch direction is up to 3.07nrad; the maximum value of vibration level decreases by 103.62 dB.

Table 3
The RMS value of angular displacement of four-axis flexure hinge in the pitch direction.

Method	Uncontrolled	FuLMS	FuLMS-ADRC
RMS (nrad)	352.24	63.30	3.07

Table 4
The maximum value of vibration level under random disturbance.

Method	Uncontrolled	FuLMS	FuLMS-ADRC
Vibration Level (dB)	−91.68	−108.4	−195.3

Table 5
PSD values at important frequencies.

Frequency (Hz)	Uncontrolled dBm/Hz	FuLMS dBm/Hz	FuLMS-ADRC dBm/Hz
38.38	−86.299	−140.784	−189.674
51.60	−86.082	−135.432	−197.443
64.30	−86.740	−132.276	−202.796
452.00	−75.193	−89.908	−229.847

The frequency-domain signal displacement of four-axis flexure hinge in the pitch direction is shown in Fig. 10. PSD values at important frequencies are shown in Table 5. Obviously, with the active vibration control method based on FuLMS-ADRC hybrid algorithm, the displacement signal PSD of four-axis flexure hinge in the pitch direction shows obvious downward trend; in particular, the PSD at natural frequency of 452 Hz decreased by 154.654 dBm/Hz.

3.2. *Short-time fourier analysis*

Short time Fourier transform can observe the time-varying spectrum signal, which is often used in non-stationary signal analysis. The short-time Fourier analysis results of displacement signal of four-axis flexure

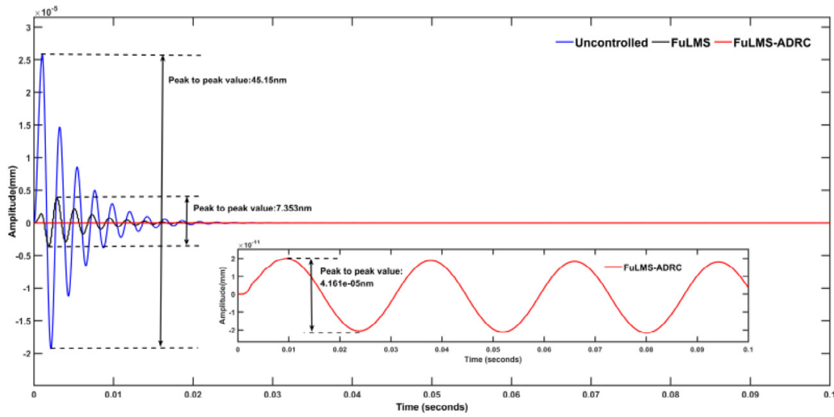

Fig. 7. Displacement signal of four-axis flexure hinge in the pitch direction under step-disturbance.

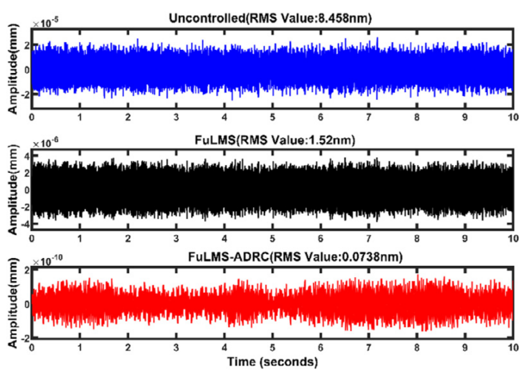

Fig. 8. Time-domain results.

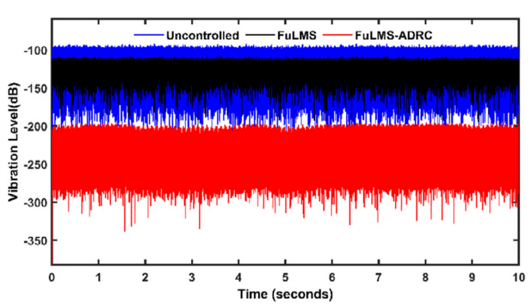

Fig. 9. The vibration level of displacement signal under random disturbance.

hinge in the pitch direction are shown in Fig. 11. Intuitively, with the active vibration control method based on FuLMS-ADRC algorithm, the short-time Fourier spectrum of displacement signal gradually cools down and the signal energy attenuates obviously. In particular, the formants at frequencies 38.38 Hz, 51.60 Hz, 64.30 Hz and 452 Hz show obvious attenuation effect.

4. Conclusion

In this work, we propose a new active vibration control method based on FuLMS-ADRC hybrid algorithm. It is found that the RMS value of angular displacement of four-axis flexure hinge in the pitch direction can be reduced to 3.07 nrad by this active vibration control method under LN_2 cooling cycle. In particular, the PSD of displacement signal at work frequency and natural frequencies is greatly attenuated. From the perspective of short-time Fourier analysis, we find that the active control method based on FuLMS-ADRC hybrid algorithm shows ideal vibration reduction effect. It can be seen that the active vibration control method is effective and can ensure the stability index of DCM under LN_2 working condition.

It is worth noting that this active control method can reduce the angular displacement RMS value of the flexure hinge in the pitch direction to about 3nrad. However, the angle stability of the actual DCM needs further engineering practice. Under the current stability requirements of DCM, the active control method based on FuLMS-ADRC hybrid algorithm provides a highly innovative technical method for the synchrotron radiation facilities of the world, which is of great significance to realize the ultra-high stability index of DCM.

CRediT authorship contribution statement

Bai Yang: Dynamic Modeling and Simulation of Flexure Hinges, FxLMS-AVC system design and optimization, Writing – original draft. **Gong Xuepeng:** Guide for thesis writing, Flexure Hinges design, Writing – review & editing. **Lu Qipeng:** Writing – review & editing. **Song Yuan:** Writing – review & editing. **Wang Dazhuang:** Data acquisition. **Peng Zhongqi:** Writing – review & editing. **Zhang Zhen:** Data analysis. **Mao Qijun:** Data analysis. **Ma Tianyu:** Data analysis.

Declaration of competing interest

The authors declare that they have no known competing financial interests or personal relationships that could have appeared to influence the work reported in this paper.

Acknowledgments

The work is supported by National Natural Science Foundation of China (No. 61974142, No. 62104224) and “Xu-Guang” Talent Program of Changchun Institute of Optics, Fine Mechanics and Physics (CIOMP), China, Chinese Academy of Sciences (CAS) (E01672Y6Q0). The Open Fund of State Key Laboratory of Applied Optics (No. SKLAO2020001A09).

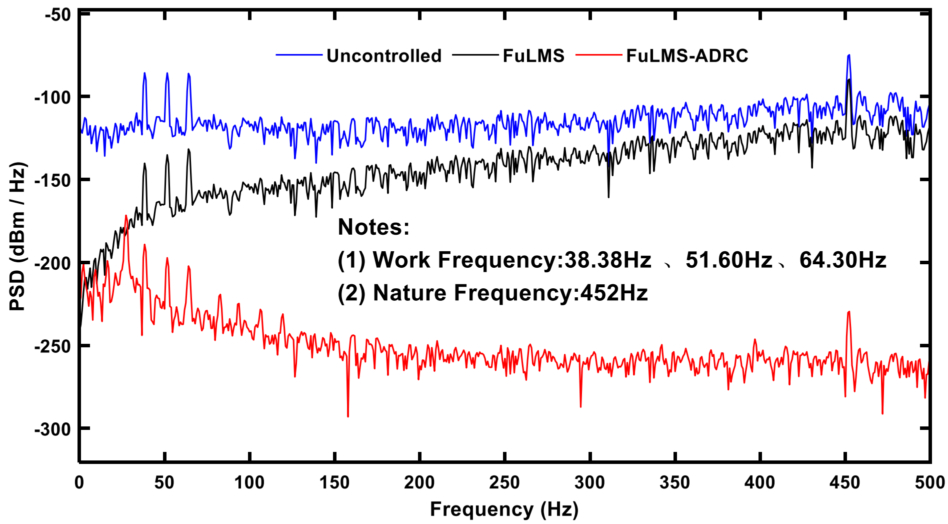

Fig. 10. Frequency-domain results.

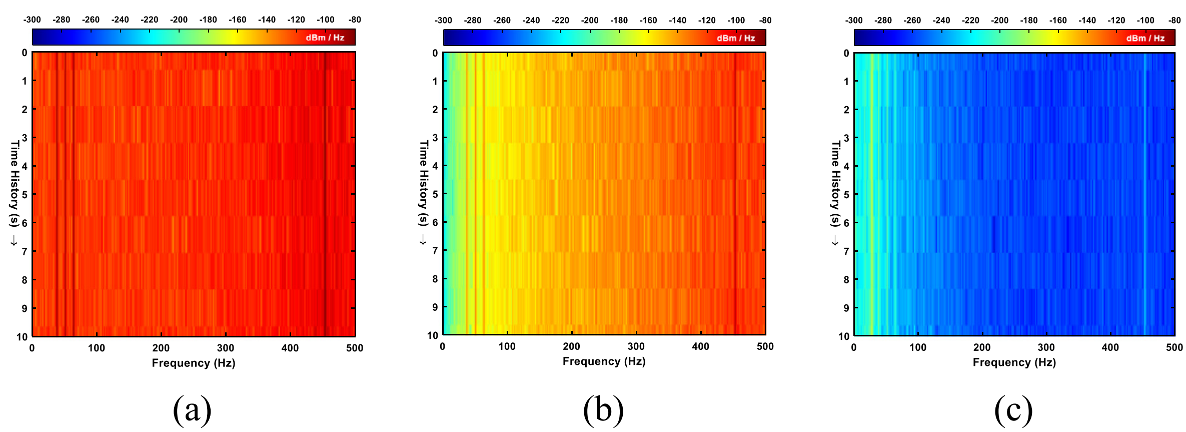

Fig. 11. The short-time Fourier analysis results of displacement signal of four-axis flexure hinge in the pitch direction. (a) Uncontrolled (b) FuLMS (c) FuLMS-ADRC.

References

[1] R.M. Galiari, et al., Studies on flow-include-vibration for the new high-dynamics DCM for Sirius presented at MEDSI 2016, 2016, Barcelona, Spain.
[2] H. Yamazaki, H. Ohashi, Y. Senba, et al., Improvement in stability of Spring-8 X-ray monochromators with cryogenic-cooled silicon crystals, J. Phys. Conf. Ser. (2013).
[3] Roland Barrett, et al., New generation mirror systems for the ESRF upgrade beam lines[c], J. Phys. Conf. Series. (2013).
[4] Wu. Jiaxing, Gong. Xuepeng, et al., Improvement of the performance of a cryo-cooled monochromator at SSRF.Part I:Double-crystal parallelism, Nucl. Inst. Methods Phys. Res. (2021).
[5] Wu. Jiaxing, Gong. Xuepeng, et al., Improvement of the performance of a cryo-cooled monochromator at SSRF.Part II: Angular stability of the exit beam, Nucl. Inst. Methods Phys. Res. (2021).
[6] Y.U. Dongchen, Structural Vibration Analysis [M], Jilin university of China Press, Changchun, 2008, 7. (In Chinese).
[7] L.J. ERIKSSON, Development of the filtered-U algorithm for active noise control, J. Acoust. Soc. Am. (1991) 89.
[8] Li. Shengquan, et al., Multi-mode active vibration control of reinforcement plate structure based on output estimated ADRC strategy, J. Vib. Eng. 25 (1) (2012) (In Chinese).
[9] Stability test report of DCM in P2 beam line station of SSRF[r], 2020, 3.